

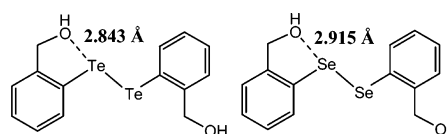
***o*-Hydroxymethylphenylchalcogens: Synthesis, Intramolecular Nonbonded Chalcogen...OH Interactions, and Glutathione Peroxidase-like Activity**

Santosh K. Tripathi,[†] Upali Patel,[†] Dipankar Roy,[†] Raghavan B. Sunoj,[†] Harkesh B. Singh,^{*,†} Gotthelf Wolmershäuser,[‡] and Ray J. Butcher[§]

Department of Chemistry, Indian Institute of Technology, Bombay, Powai, 400076 Mumbai, India, Fachbereich Chemie, Universität Kaiserslautern, Postfach 3049, Kaiserslautern 67653, Germany, and Department of Chemistry, Howard University, Washington D.C. 20059

chhbsia@chem.iitb.ac.in

Received June 27, 2005



mPW1PW91/LanL2DZdp, 6-311G**

NBO: $E(\text{chalcogen}\cdots\text{O})$

AIM: $\rho(\text{chalcogen}\cdots\text{O})_{\text{bcp}}$

Experimental: $(\text{chalcogen}\cdots\text{O})_{\text{distance}}$

22

8.75 kcal/mol

0.022 ea_0^{-3}

3.021 Å

15

4.04 kcal/mol

0.016 ea_0^{-3}

3.008 Å

The synthesis and characterization of a series of organochalcogen (Se, Te) compounds derived from benzyl alcohol **13** are described. The synthesis of the key precursor dichalcogenides **15**, **22**, and **29** was achieved by the *ortho*-lithiation route. Selenide **18** was obtained by the reaction of the dilithiated derivative **14** with $\text{Se}(\text{dte})_2$. Oxidation of **15** and **22** with H_2O_2 afforded the corresponding cyclic ester derivatives **17** and **24**, respectively. Oxidation of selenide **18** with H_2O_2 affords the spirocyclic compound **19**. The presence of intramolecular interactions in dichalcogenides **15** and **22** has been proven by single-crystal X-ray studies. The cyclic compounds **17** and **19** have also been characterized by single-crystal X-ray studies. GP_X-like antioxidant activity of selenium compounds has been evaluated by the coupled bioassay method. Density functional theory calculations at the mPW1PW91 level on ditelluride **22** have identified a fairly strong nonbonding interaction between the hydroxy oxygen and tellurium atom. The second-order perturbation energy obtained through NBO analysis conveys the involvement of $n_{\text{O}} \rightarrow \sigma^*_{\text{Te}-\text{Te}}$ orbital overlap in nonbonding interaction. Post wave function analysis with the Atoms in Molecules (AIM) method identified distinct bond critical point in **15** and **22** and also indicated that the nonbonding interaction is predominantly covalent. Comparison between diselenide **15** and ditelluride **22** using the extent of orbital interaction as well as the value of electron density at the bond critical points unequivocally established that a ditelluride could be a better acceptor in nonbonding interaction, when the hydroxy group acts as the donor.

Introduction

Organochalcogen compounds having intramolecular E...X interactions (where E = Se, Te; X = N, O) play a very important role in the areas of organic synthesis,¹ enzyme mimetics,² ligand chemistry,³ and isolation of metal organic chemical vapor deposition (MOCVD) precursors.⁴ We and others have reported the synthesis and structural characterization of a variety of intramolecularly coordinated organochalcogens where the coordinating atoms are N, O, and H.^{5,6} The nature of these

nonbonded interactions has been thoroughly investigated by single-crystal X-ray diffraction, detailed multinuclear NMR, and theoretical studies. The coordinating groups generally include tertiary amine, azo, azomethine, py-

(1) Reviews: (a) *Organoselenium Chemistry: A Practical Approach*; Back, T. G., Ed.; Oxford University Press: New York, 1999. (b) Wirth, T. *Tetrahedron* **1999**, *55*, 1. (c) Wirth, T. *Angew. Chem., Int. Ed.* **2000**, *39*, 3740. (d) *Organoselenium Chemistry: Modern Development in Organic Synthesis*; Wirth, T., Ed.; Springer-Verlag: Berlin, Germany, 2000. (e) Nishibayashi, Y.; Uemura, S. *Top. Curr. Chem.* **2000**, *208*, 201. Also see: (f) Uehlin, L.; Wirth, T. *Org. Lett.* **2001**, *3*, 2931. (h) Back, T. G.; Moussa, Z.; Parvez, M. *J. Org. Chem.* **2002**, *67*, 499. (j) Tiecco, M.; Testaferri, L.; Santi, C.; Tomassini, C.; Marini, F.; Bagnoli, L.; Temperini, A. *Chem. Eur. J.* **2002**, *8*, 1118. (k) Uehlin, L.; Fragale, G.; Wirth, T. *Chem. Eur. J.* **2002**, *8*, 1125. (l) Tiecco, M.; Testaferri, L.; Santi, C.; Tomassini, C.; Marini, F.; Bagnoli, L.; Temperini, A. *Angew. Chem., Int. Ed.* **2003**, *42*, 3131. (m) Khokhar, S. S.; Wirth, T. *Angew. Chem., Int. Ed.* **2004**, *43*, 631.

* To whom correspondence should be addressed. Tel: (22) 2576 7190. Fax: (22) 2572 3480.

[†] Indian Institute of Technology.

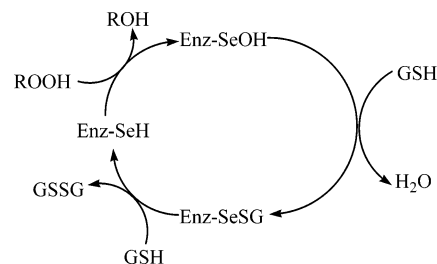
[‡] Universität Kaiserslautern.

[§] Howard University.

ridyl, oxazoline, oxazine, and carbonyl groups. There are very few studies involving the coordinating hydroxy, ether, and halogen groups. The notable exception is the pioneering work of Tomoda and co-workers, where intramolecular Se...OH, Se...OR, and Se...halogen interactions have been systematically investigated mainly by multinuclear NMR and theoretical studies (1–3).⁷ However, there are no reports on structural characterization of E...OH interactions in the solid state.

The organochalcogens with an *o*-hydroxy function (or hydroxy group present in close proximity) have attracted attention due to their relevance (i) in organic synthesis,⁸ (ii) in biochemistry,⁹ (iii) as intermediates in the catalytic cycle of seleninate esters,¹⁰ (iv) as precursors for GPx

SCHEME 1



mimics,¹⁰ and (v) as hydroxy-containing mimics have better solubility in water for conducting the bioassay.¹¹ Wirth and co-workers⁸ have demonstrated the use of **4** and related diselenides in stereoselective selenenylation reactions. An intramolecular Se...O interaction is necessary for high diastereoselectivity. The diselenides with a free hydroxy group give the highest diastereoselectivity. Interestingly, the single-crystal structure of **4b** does not show Se...OH interaction. Instead, it shows Se...OME interaction.

The discovery of selenium as selenocysteine in the active site of the selenoenzyme glutathione peroxidase (GPx) has led to a growing interest in the biochemistry of selenium.¹² The selenoenzyme functions as an antioxidant and catalyzes the reduction of harmful peroxides by glutathione and protects the lipid membranes against oxidative damage.¹³ The enzyme's catalytic site includes a selenocysteine residue in which the selenium undergoes a redox cycle involving the selenol (Enz-SeH) as the active form that reduces hydroperoxides and organic peroxides. The selenol is oxidized to the selenenic acid (Enz-SeOH), which reacts with reduced glutathione (GSH) to form the selenenyl sulfide adduct (Enz-SeSG). A second glutathione then regenerates the active form of the enzyme by attacking the sulfide to form the oxidized glutathione (GSSG) (Scheme 1).¹⁴

Simple organoselenium compounds have been shown to mimic the GPx activity in vitro. These include ebselen (2-phenyl-1,2-benzoselenazol-3-(2*H*)-one **5**),¹⁵ ebselen analogues,¹⁶ benzoselenazolinones,¹⁷ selenamide and related derivatives,¹⁸ diaryl diselenides **6** and **7**,^{2a,f,g,19} various tellurides and ditellurides,^{2c,5b,20} and the semi-

(2) (a) Wilson, S. R.; Zucker, P. A.; Huang, R.-R. C.; Spector, A. *J. Am. Chem. Soc.* **1989**, *111*, 5936. (b) Spector, A.; Wilson, S. R.; Zucker, P. A. U.S. Patent 5,321,138 (C1, 546–224; C07C37/02), 1994; *Chem. Abstr.* **1994**, *121*, P256039r. (c) Engman, L.; Stern, D.; Cotgreave, I. A.; Andersson, C. M. *J. Am. Chem. Soc.* **1992**, *114*, 9737. (d) Galet, V.; Bernier, J.-L.; Henichart, J.-P.; Lesieur, D.; Abadie, C.; Rochette, L.; Lindenbaum, A.; Chalas, J.; Faverie, J.-F. R.; Pfeiffer, B.; Renard, P. *J. Med. Chem.* **1994**, *37*, 2903. (e) Iwaoka, M.; Tomoda, S. *J. Am. Chem. Soc.* **1994**, *116*, 2557. (f) Mughesh, G.; Panda, A.; Singh, H. B.; Punekar, N. S.; Butcher, R. J. *Chem. Commun.* **1998**, 2227. (g) Mughesh, G.; Panda, A.; Singh, H. B.; Punekar, N. S.; Butcher, R. J. *J. Am. Chem. Soc.* **2001**, *123*, 839. (h) Mughesh, G.; du Mont, W.-W. *Chem. Eur. J.* **2001**, *7*, 1365.

(3) (a) Singh, A. K.; Sharma, S. *Coord. Chem. Rev.* **2000**, *209*, 49. (b) Levason, W.; Orchard, S. D.; Reid, G. *Coord. Chem. Rev.* **2002**, *225*, 159. (c) Iwaoka, M.; Tomoda, S. *J. Chem. Soc., Chem. Commun.* **1992**, 1165. (d) Fujita, K.; Iwaoka, M.; Tomoda, S. *Chem. Lett.* **1994**, 923. (e) Wirth, T. *Tetrahedron Lett.* **1995**, *36*, 7849. (f) Kaur, R.; Singh, H. B.; Patel, R. P. *J. Chem. Soc., Dalton Trans.* **1996**, 2719. (g) Fukuzawa, S.; Takahashi, K.; Kato, H.; Yamazaki, H. *J. Org. Chem.* **1997**, *62*, 7711. (h) Wirth, T.; Hauptli, H.; Leuenberger, M. *Tetrahedron: Asymmetry* **1998**, *9*, 547. (i) Uemura, S. *Phosphorus, Sulfur Silicon Relat. Elem.* **1998**, *136–138*, 219. (j) Hiroi, K.; Suzuki, Y.; Abe, I. *Tetrahedron: Asymmetry* **1999**, *10*, 1173. (k) Ehara, H.; Noguchi, M.; Sayama, S.; Onami, T. *J. Chem. Soc., Perkin Trans. I* **2002**, 1429. (l) Braga, A. L.; Paixao, M. W.; Ludtke, D. S.; Silveira, C. C.; Rodrigues, O. E. *D. Org. Lett.* **2003**, *5*, 2635.

(4) (a) Bonasia, P. J.; Arnold, J. J. *Organomet. Chem.* **1993**, *449*, 147. (b) Cheng, Y.; Emge, T. J.; Brennan, G. *Inorg. Chem.* **1994**, *33*, 3711. (c) Cheng, Y.; Emge, T. J.; Brennan, G. *Inorg. Chem.* **1996**, *35*, 3342. (d) Cheng, Y.; Emge, T. J.; Brennan, G. *Inorg. Chem.* **1996**, *35*, 7339. (e) Mughesh, G.; Singh, H. B.; Butcher, R. J. *Inorg. Chem.* **1998**, *37*, 2663. (f) Mughesh, G.; Singh, H. B.; Butcher, R. J. *J. Organomet. Chem.* **1999**, *577*, 243. (g) Kandasamy, K.; Singh, H. B.; Wolmershäuser, G. *Inorg. Chim. Acta* **2005**, *358*, 207.

(5) (a) Mughesh, G.; Singh, H. B. *Acc. Chem. Res.* **2002**, *35*, 226. (b) Mughesh, G.; Panda, A.; Kumar, S.; Apte, S. D.; Singh, H. B.; Butcher, R. J. *Organometallics* **2002**, *21*, 884. (c) Kandasamy, K.; Kumar, S.; Singh, H. B.; Wolmershäuser, G. *Organometallics* **2003**, *22*, 5069. (d) Apte, S. D.; Zade, S. S.; Singh, H. B.; Butcher, R. J. *Organometallics* **2003**, *22*, 5473. (e) Kumar, S.; Kandasamy, K.; Singh, H. B.; Wolmershäuser, G.; Butcher, R. J. *Organometallics* **2004**, *23*, 4199. (f) Zade, S. S.; Singh, H. B.; Butcher, R. J. *Angew. Chem., Int. Ed.* **2004**, *43*, 4513. (g) Zade, S. S.; Panda, S.; Tripathi, S. K.; Singh, H. B.; Wolmershäuser, G. *Eur. J. Org. Chem.* **2004**, *18*, 3857. (h) Kumar, S.; Kandasamy, K.; Singh, H. B.; Butcher, R. J. *New J. Chem.* **2004**, *28*, 640. (i) Kandasamy, K.; Kumar, S.; Singh, H. B.; Butcher, R. J.; Holman, K. T. *Organometallics* **2004**, *5*, 1014. (j) Zade, S. S.; Panda, S.; Singh, H. B.; Sunoj, R. B.; Butcher, R. J. *J. Org. Chem.* **2005**, *70*, 3693.

(6) (a) Goldstein, B. M.; Kennedy, S. D.; Hennen, W. J. *J. Am. Chem. Soc.* **1990**, *112*, 8265. (b) Burling, F. T.; Goldstein, B. M. *J. Am. Chem. Soc.* **1992**, *114*, 2313. (c) Barton, D. H. R.; Hall, M. B.; Lin, Z.; Parekh, S. I.; Reibenspies, J. J. *J. Am. Chem. Soc.* **1993**, *115*, 5056. (d) Fujihara, H.; Mima, H.; Furukawa, N. *J. Am. Chem. Soc.* **1995**, *117*, 10153. (e) Furukawa, N.; Kobayashi, K.; Sato, S. *J. Organomet. Chem.* **2000**, *611*, 116 and references therein. (f) Nakanishi, W.; Hayashi, S.; Itoh, N. *Chem. Commun.* **2003**, 124 and references therein. (g) Klapötke, T. M.; Krumm, B.; Polborn, K. *J. Am. Chem. Soc.* **2004**, *126*, 710. (h) Nakanishi, W.; Hayashi, S.; Itoh, N. *J. Org. Chem.* **2004**, *69*, 1676.

(7) (a) Komatsu, H.; Iwaoka, M.; Tomoda, S. *Chem. Commun.* **1999**, 2, 205. (b) Iwaoka, M.; Katsuda, T.; Tomoda, S.; Harada, J.; Ogawa, K. *Chem. Lett.* **2002**, *5*, 518. (c) Iwaoka, M.; Takemoto, S.; Tomoda, S. *J. Am. Chem. Soc.* **2002**, *124*, 0613. (d) Iwaoka, M.; Komatsu, H.; Katsuda, T.; Tomoda, S. *J. Am. Chem. Soc.* **2004**, *126*, 5309. (e) Iwaoka, M.; Takayuki, K.; Hiroto, K.; Tomoda, S. *J. Org. Chem.* **2005**, *70*, 321.

(8) (a) Wirth, T.; Fragale, G.; *Chem. Eur. J.* **1997**, *3*, 1894. (b) Fragale, G.; Neuberger, M.; Wirth, T. *Chem. Commun.* **1998**, 1867.

(9) Wirth, T. *Molecules* **1998**, *3*, 164.

(10) (a) Back, T. G.; Moussa, Z. *J. Am. Chem. Soc.* **2002**, *124*, 12104.

(b) Back, T. G.; Moussa, Z. *J. Am. Chem. Soc.* **2003**, *125*, 13455.

(11) Iwaoka, M.; Takahashi, T.; Tomoda, S. *Heteroatom Chem.* **2001**, *12*, 293.

(12) (a) Rotruck, J. T.; Pope, A. L.; Ganther, H. E.; Swanson, A. B.; Hafeman, D. G. *Science* **1973**, *179*, 588. (b) Flohë, L.; Gunzler, W. A.; Schock, H. H. *FEBS Lett.* **1973**, *32*, 132.

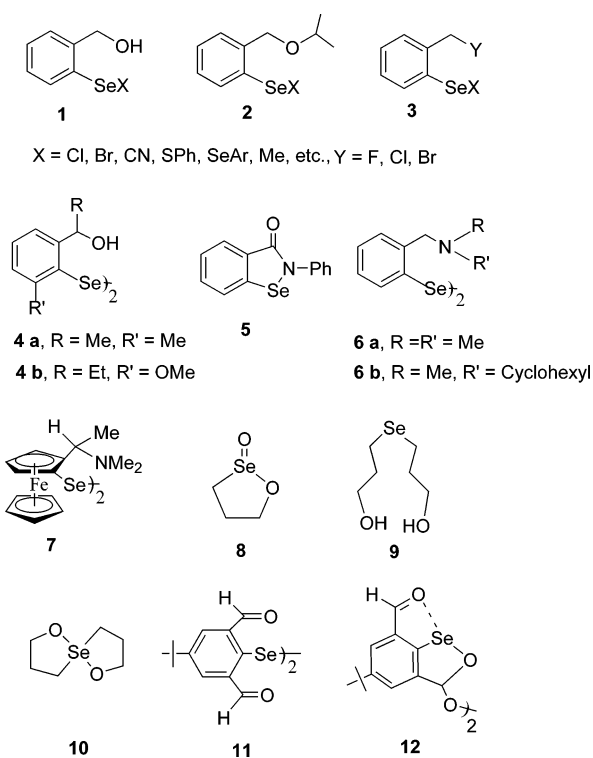
(13) (a) Mughesh, G.; du Mont, W. W.; Sies, H. *Chem. Rev.* **2001**, *101*, 2125. (b) Mughesh, G.; Singh, H. B. *Chem. Soc. Rev.* **2000**, *29*, 347. (c) *Selenium in Biology and Human Health*; Burk, R. F., Ed.; Springer: New York, 1994. (d) Flohë, L. *Curr. Top. Cell Regul.* **1985**, *27*, 473. (e) Tappel, A. L. *Curr. Top. Cell Regul.* **1984**, *24*, 87. (f) Epp, O.; Ladenstein, R.; Wendel, A. *Eur. J. Biochem.* **1983**, *133*, 51. (g) Flohë, L.; Loschen, G.; Gunzler, W. A.; Eichele, E. *Hoppe-Seyler's Z. Physiol. Chem.* **1972**, *353*, 987.

(14) Ganther, H. E. *Chem. Scr.* **1975**, *8a*, 79. (b) Ganther, H. E.; Kraus, R. J. In *Methods in Enzymology*; Colowick, S. P., Kaplan, N. O., Eds.; Academic Press: New York, 1984; Vol. 107, pp 593–602.

(15) (a) Müller, A.; Cadenas, E.; Graf, P.; Sies, H. *Biochem. Pharmacol.* **1984**, *33*, 3235. (b) Wendel, A.; Fausel, M.; Safayhi, H.; Tiegs, G.; Otter, R. *Biochem. Pharmacol.* **1984**, *33*, 3241. (c) Parnham, M. J.; Kindt, S. *Biochem. Pharmacol.* **1984**, *33*, 3247. (d) Wendel, A. European Patent 0-165-534, **1985**.

synthetic enzyme selenosubtilisin.²¹ The diselenides containing basic amino groups have attracted much attention as GPx mimics because the Se...N intramolecular nonbonded interactions (i) activate the Se...Se bond toward the oxidative cleavage, (ii) stabilize the resulting selenenic acid intermediate against further oxidation, and (iii) enhance the nucleophilic attack of the thiol at the sulfur rather than selenium compared with unsubstituted phenylselenenyl sulfide. Wirth reported, for the first time, the glutathione peroxidase-like activity of the new class of diselenides **4** containing an oxygen atom in close proximity to the selenium.⁹ Recently, Back et al.¹⁰ reported remarkable activity of a novel cyclic seleninate ester **8** with a Se–O bond as a GPx mimetic. Ester **8** was derived from allyl 3-hydroxypropyl selenide. In a more recent study, the same group²² has found that di(3-hydroxypropyl) selenide **9** exhibited exceptional GPx-like activity through intermediate spirodioxaselenanone **10**.

In continuation of our work on intramolecularly coordinated organochalcogens with nitrogen donors,⁵ we recently reported intramolecular Se...O (formyl oxygen) interaction and GPx-like activity of diselenides having two ortho oxygens and a novel seleninate ester **11**, **12**.^{5f,h} In this paper, we extend this work and report the synthesis and first structural characterization of diaryl dichalcogenides (chalcogen = Se or Te) having hydroxy groups in close proximity to the selenium atom, their novel oxidized derivatives, and GPx-like activities. The reaction mechanism and the intermediates involved in the GPx catalytic cycle have been investigated by ⁷⁷Se NMR spectroscopic studies. Also, we present herein the first theoretical investigations on Te...OH, Te...OR (phenoxy), and Te...Cl intramolecular interactions and compare the same with the corresponding selenium analogues.



Results and Discussion

The key precursor diselenide **15**²³ was prepared by the well-established *ortho*-lithiation^{8,24} route (Scheme 2). Attempted reaction of **15** with thionyl chloride to get bis(chloromethylbenzyl) diselenide, in our hands, afforded known 6*H*,12*H*-dibenzo[*b,f*][1,5]diselenocin.²⁵ The synthesis of the allyl selenide **16** was approached by the reduction of **15** with sodium borohydride followed by quenching of the in situ generated sodium selenolate with allyl bromide. Synthesis of the cyclic seleninate ester **17** was accomplished by following the method reported by Back et al. by reacting **16** with *tert*-butyl hydroperoxide (TBHP).¹⁰ Compound **17** could be alternatively prepared directly from **15** by its oxidation with an excess of H₂O₂. Compound **18** was obtained by the reaction of the *ortho*-lithiated product **14** with selenium(II) diethyldithiocarbamate [Se(dtc)₂].²⁶ Oxidation of **18** with H₂O₂ afforded **19** in almost quantitative yield. Selenenyl sulfide **20** was successfully obtained by the reaction of cyclic seleninate ester **17** with an excess (3-fold) of pentanethiol and was purified by preparative chromatography using hexane/dichloromethane (1:1) to give a pale yellow viscous oil. Compound **20** disproportionates on keeping in solution at room temperature to the corresponding diselenide and disulfide. Similarly, selenenyl sulfide **21** was generated in situ by the reaction of compound **16** with an excess (4-fold) of PhSH (Scheme 5). Attempted isolation of **21** led to its disproportionation to the corresponding diselenide and disulfide. However, the selenenyl sulfides were stable enough for characterization in solution by ¹H, ¹³C, and ⁷⁷Se NMR spectroscopy. The synthesis of tellurium compounds is depicted in Schemes 3 and 4. Attempts to prepare the tellurium analogue of **18** by the reaction of **14** with TeI₂ led to isolation of a liquid of indefinite composition.

Glutathione Peroxidase-like Activity. GPx-like activities of the selenium compounds were determined by the coupled reductase assay.²⁷ In this assay, the GPx activity was measured by a coupled enzyme system containing glutathione reductase (0.6 unit), GSH (1 mM), NADPH (0.1 mM), catalyst (0.025 mM), and TBHP (1.2

(16) (a) Jacquemin, P. V.; Christiaens, L. E.; Renson, M. J.; Evers, M. J.; Dereu, N. *Tetrahedron Lett.* **1992**, *33*, 3863. (b) Zade, S. S.; Panda, S.; Tripathi, S. K.; Singh, H. B.; Wolmershaeuser, G. E. *J. Org. Chem.* **2004**, *18*, 3857.

(17) Galet, V.; Bernier, J.-L.; Henichart, J.-P.; Lesieur, D.; Abadie, C.; Rochette, L.; Lindenbaum, A.; Chalas, J.; Renaud de la Faverie, J. F.; Pfeiffer, B.; Renard, P. *J. Med. Chem.* **1994**, *37*, 2903.

(18) (a) Back, T. G.; Dyck, B. P. *J. Am. Chem. Soc.* **1997**, *119*, 2079. (b) Reich, H. J.; Jaspers, C. P. *J. Am. Chem. Soc.* **1987**, *109*, 5549.

(19) Zhang, X.; Xu, H.; Dong, Z.; Wang, Y.; Liu, J.; Shen, J. *J. Am. Chem. Soc.* **2004**, *126*, 10556.

(20) (a) You, Y.; Ahsan, K.; Detty, M. R. *J. Am. Chem. Soc.* **2003**, *125*, 4918. (d) Engman, L.; Stern, D.; Pelcman, M.; Andersson, C. M. *J. Org. Chem.* **1994**, *59*, 1973. (e) Vessman, K.; Ekstorm, M.; Verglund, M.; Andersson, C. M.; Engman, L. *J. Org. Chem.* **1995**, *60*, 4461.

(21) (a) Wu, Z.-P.; Hilvert, D. *J. Am. Chem. Soc.* **1989**, *111*, 4513. (b) Wu, Z.-P.; Hilvert, D. *J. Am. Chem. Soc.* **1990**, *112*, 5647.

(22) Back T. G.; Moussa Z. *Angew. Chem., Int. Ed.* **2004**, *43*, 1268

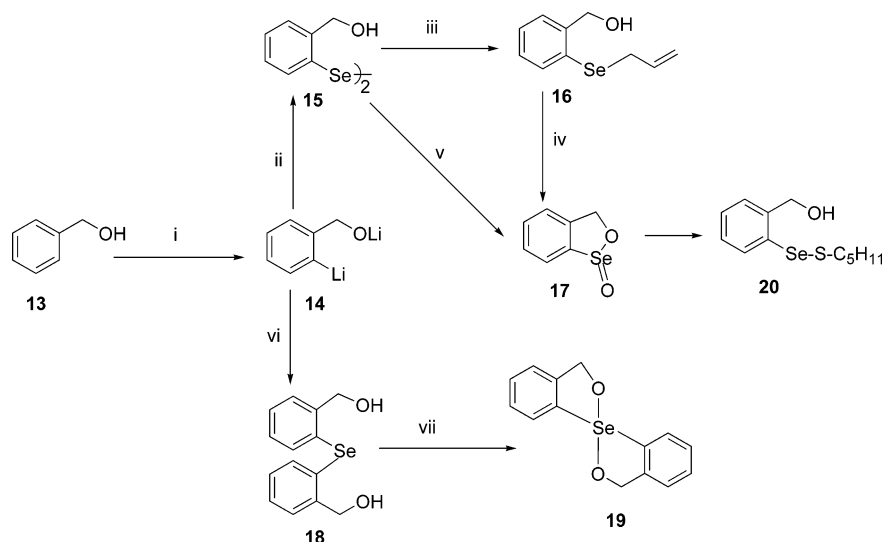
(23) Iwaoka, M.; Tomoda, S. *Phosphorus, Sulfur Silicon Relat. Elem.* **1992**, *67*, 125.

(24) (a) Rickard, C. E. F.; Roper, W. R.; Tutone, F.; Woodgate, S. D.; Wright, L. J. *J. Organomet. Chem.* **2001**, *619*, 293. (b) Constantinos, S. S.; Ioannis D. K.; Maria, M.; George, A. H.; Constantinos, G. S. *J. Org. Chem.* **1996**, *64*, 5589.

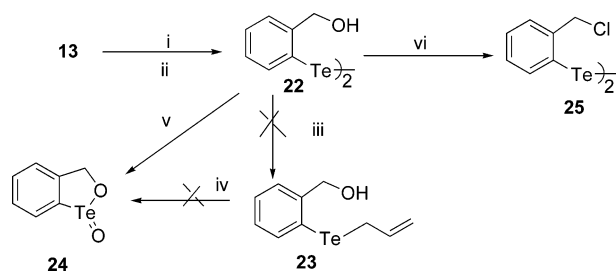
(25) Iwaoka, M.; Tomoda, S. *J. Am. Chem. Soc.* **1994**, *116*, 4463.

(26) Foss, O. *Inorg. Synth.* **1953**, *4*, 91.

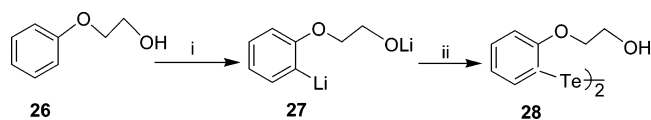
(27) Kumar, S.; Panda, S.; Singh, H. B.; Wolmershaeuser, G.; Butcher, R. J. *J. Struct. Chem.*, in press.

SCHEME 2^a

^a Reagents and conditions: (i) *n*-BuLi, TEMDA, pentane; (ii) Se/THF; (iii) NaBH₄, C₃H₅Br; (iv) TBHP; (v) H₂O₂; (vi) Se(dtc)₂; (vii) H₂O₂/AcOH.

SCHEME 3^a

^a Reagents and conditions: (i) *n*-BuLi, TMEDA, pentane; (ii) Te/THF; (iii) NaBH₄, C₃H₅Br; (iv) TBHP; (v) H₂O₂; (vi) SOCl₂

SCHEME 4^a

^a Reagents and conditions: (i) *n*-BuLi, pentane/-78 °C; (ii) Te/THF/O.

mM). The reduction of TBHP by GSH was also carried out using ebselen **5** and seleninate ester **8** for comparison. The decrease in NADPH concentration was monitored spectrophotometrically at 340 nm, and the results are summarized in Table 1. It was found that diselenide **15** and cyclic seleninate ester **17** are more efficient catalysts in comparison to ebselen **5** and have comparable activity to that of aliphatic seleninate ester **8**. The high activity of **15** is probably due to intramolecular Se...O nonbonding interaction [Se(2)···O(2) = 3.008 Å] (vide infra). Interestingly, bis(formylphenyl)diselenide²⁸ having a strongly coordinating carbonyl group showed relatively poor activity (entry 9) as compared to **15**, which has a weakly coordinating hydroxy group. Surprisingly, allyl selenide **16** did not show any considerable activity even when a 4-fold excess amount of the catalyst was used (entry 4). Similarly, selenide **18** also showed poor GPx activity. The

TABLE 1. Glutathione Peroxidase-like Activity of Selenium Compounds Determined by Coupled Reductase Assay

entry	catalyst	V ₀ ^a (μM/min)
1	none	1.17
2	5	8.63
6	8	5.18
3	15	30.02
4	16	–
5	17	26.5
7	18	1.41
8	19	14.9
9	bis(2-formylphenyl)Se ₂ ²⁸	12.07

^a Moles of NADPH utilized per minute.

spirocyclic compound **19** where selenium is in oxidation state IV was less active than the seleninate ester **17**.

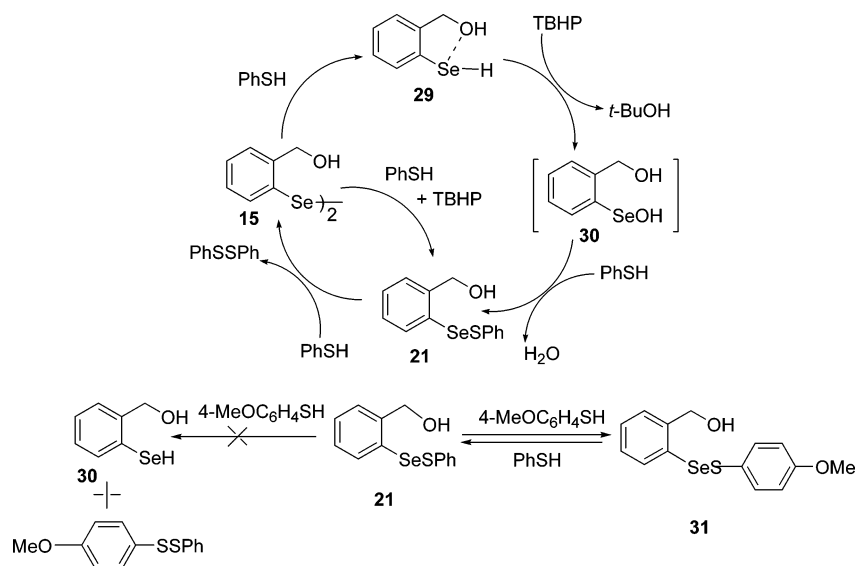
GPx-like activities of the tellurium analogues **22**, **24**, **25**, and **28** were also evaluated by coupled reductase assay. During the assay, an immediate formation of a precipitate was observed soon after the addition of benzenethiol to the reaction mixture, and therefore, the obtained values are not satisfactory.

Mechanism. To understand the mechanism and identify the intermediates involved in the peroxidase reaction we next set out to use ⁷⁷Se NMR spectroscopy since its chemical shift is very sensitive to the environment. Moreover, all three major intermediates, i.e., RSeH, RSeOH, and RSeSPh, are expected to show large differences in their chemical shift values. The model reactions were monitored by ⁷⁷Se NMR for 0–1 h. The signals generally appeared within 5–15 min and did not change positions with passage of time.

Reaction of 15 with Benzenethiol and TBHP. The 1:1 molar reaction of **15** (413 ppm) with PhSH did not show signals corresponding to the expected selenenyl sulfide **21** and selenol **29**, indicating that the initial reaction was too slow. However, when a second equivalent of PhSH was added, two signals at 199.5 and 413 ppm due to selenol **29** and diselenide **15**, respectively, were observed. There is a downfield shift of ~54.5 ppm

(28) Wendel, A. *Methods Enzymol.* **1981**, *77*, 325.

SCHEME 5



of ⁷⁷Se NMR for **29** compared with the chemical shift of benzeneselenol (145 ppm).²⁹ This downfield shift is due to strong intramolecular interaction between Se and O atom.

When an equimolar amount of TBHP was added to the reaction mixture containing selenol **29**, two signals at 414 and 495 ppm were observed due to formation of diselenide **15** and selenenyl sulfide **21**, respectively. When **15** was treated with both PhSH and TBHP simultaneously, two signals were observed at 414 and 495 ppm corresponding to **15** and **21**, respectively, and no signal due to selenenic acid **30** (vide infra) was observed. This is probably due to its fast conversion to selenenyl sulfide. Selenenic acid **30** and other more oxidized products were not detected even after the addition of an excess of TBHP indicating high stability of the selenenyl sulfide.

In conclusion, the reaction of diselenide **15** with 1 equiv of TBHP and PhSH leads to the rapid formation of selenenyl sulfide **21** and diselenide **15**, and no selenol or the oxidized species are detected. However, when the reaction mixture containing selenenyl sulfide was treated with PhSH, the signal due to selenenyl sulfide disappeared completely and only one signal at 413 ppm due to diselenide **15** appeared, thus indicating that the selenenyl sulfide converts to selenol **29** which then is readily oxidized to diselenide **15** (Scheme 5). To test this hypothesis, a crossover experiment was performed in which the reaction mixture containing selenenyl sulfide **21** and diselenide **15** was treated with 4-methoxybenzenethiol. After 1 h, the ⁷⁷Se NMR spectrum of the reaction mixture showed a signal for the new selenenyl sulfide **31** (545.1 ppm) together with the original selenenyl sulfide **21** (494.6 ppm) and diselenide **15** (414.6 ppm). The formation of the selenenyl sulfide **31** could be explained by the nucleophilic attack of 4-methoxybenzenethiol directly at the selenium atom of selenenyl sulfide **21** with displacement of PhSH. The results of the crossover experiments are, therefore, consistent with the postulated reaction of selenenyl sulfide **21** with PhSH to produce selenol **29** and diphenyl disulfide.

Reaction of **17** with Benzenethiol and TBHP.

From the time of appearance of the ⁷⁷Se NMR signals, the reaction of seleninate ester **17** (1348.81 ppm) with 1 equiv of PhSH was found to be extremely slow. Reaction of seleninate ester with 2 equiv of PhSH afforded the expected signal of selenenic acid **30** (1199.92 ppm). The ⁷⁷Se NMR chemical shift is significantly downfield shifted compared with that of o-nitrobenzeneselenenic acid (1066 ppm)³⁰ but close to the value reported for the selenenic acid derived from N,N'-dimethylbenzylamine diselenide (1173 ppm) and bis(4,4'-dimethyl-2-oxazolonyl)phenyl] diselenide,^{2f} thus indicating a strong Se...O interaction in **30**. When seleninate ester was treated with an excess of TBHP, the signal due to selenenic acid completely disappeared and only one signal at 1345.8 ppm was observed, indicating that all selenenic acid had converted back to the cyclic seleninate ester. A similar reactivity has been observed by Back et al.¹⁰ in the reaction of the aliphatic selenenic acid derived from cyclic seleninate ester **8**.

Reaction of seleninate ester with a 4-fold excess of PhSH afforded the expected selenenyl sulfide **21** (506.58 ppm). The signal of selenenyl sulfide is upfield shifted by 20.58 ppm from that of PhSeSPh (526.0 ppm).³¹ Reaction of the selenenyl sulfide with an excess of TBHP did not immediately give the cyclic ester **17**, but we observed a new signal due to formation of diselenide (428.73 ppm) which may be due to disproportionation of **21** to **15**. This indicates an alternative mechanism for the oxidation of **21** to **17** via disproportionation of **21** into the corresponding diselenide **15** and PhSH (Scheme 6), followed by oxidation of **15**. The presence of the diselenide signal suggests that disproportionation of the selenenyl sulfide is a major pathway in the regeneration of **17** from **21**. We have also synthesized related selenenyl sulfide **20**

(30) Reich, H. J.; Willis, W. W.; Wollowitz, S. *Tetrahedron Lett.* **1982**, 23, 3319. (b) Goto, K.; Nagahama, M.; Mizushima, T.; Keiichi S.; Takayuki, K.; Renji, O. *Org. Lett.* **2001**, 3, 3569.

(31) (a) Luthera, N. P.; Dunlap, R. B.; Odom, J. D. *J. Magn. Reson.* **1982**, 46, 152. (b) Khoon-Sin, T.; Arnold, A. P.; Rabenstein, D. L. *Can. J. Chem.* **1988**, 66, 54.

(29) McFarlane, W.; Wood, R. J. *J. Chem. Soc. A* **1972**, 1397.

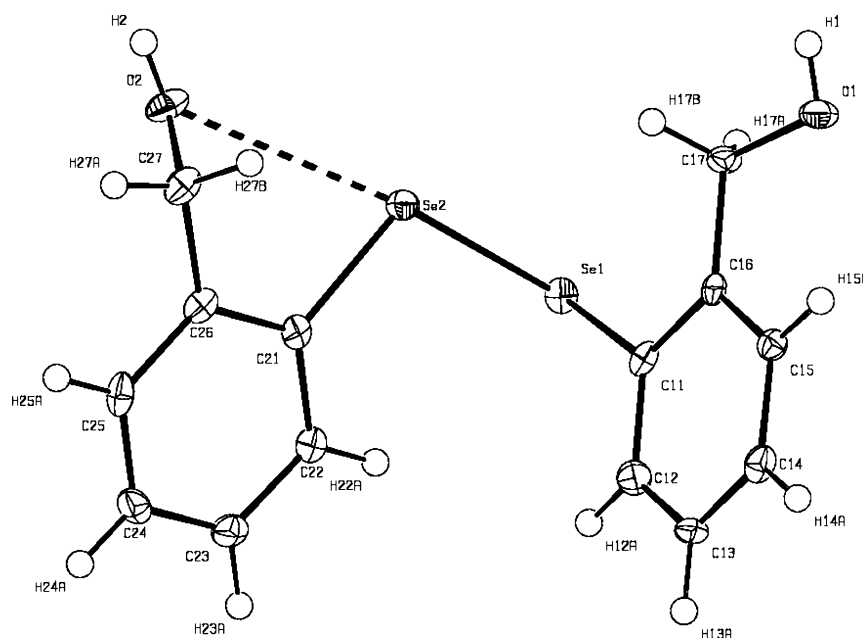
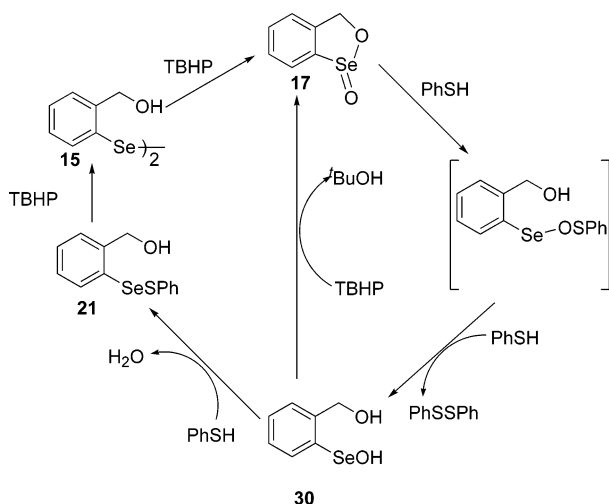


FIGURE 1. Molecular structure of 15.

SCHEME 6



(438.23 ppm) for comparison of the chemical shifts. This value is quite close to that of dibenzyl diselenide **15** (428 ppm).

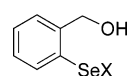
Mass spectrometric technique was also used for the characterization of the intermediates.

The mass spectrum of a mixture of the seleninate ester **17** with 1 equiv of PhSH showed three characteristic peaks due to formation of selenenic acid thiolester (**31**, $m/z = 309.8$) and other more oxidized product such as selenenic acid thiol ester **32** ($m/z 327$) and selenenic acid thiol ester **33** ($m/z 345.8$). The reaction of seleninate ester with 2 equiv of PhSH shows the formation of selenenic acid **30** ($m/z 203$). The formation of selenenic acid was also confirmed by the ^{77}Se NMR. A signal was observed at 1199.92 for the reaction of seleninate ester and 2 equiv of PhSH, other more oxidized products are also observed such as diphenyl disulfide ($m/z 218$) and selenenic acid thiol ester **33**. When we added TBHP to this reaction mixture we got back cyclic seleninate ester **17** ($m/z 202.9$) due to oxidation–dehydration of selenenic acid thiol ester

TABLE 2. Comparison of Experimentally Obtained Structural Parameters (Å and deg) with That Computed at the MPW1PW91/LanL2DZ d_p , 6-311G ** Level for Compound 15

	exptl	calcd		exptl	calcd
Se(1)–C(11)	1.934(3)	1.940	C(21)–Se(2)–Se(1)	104.40(9)	104.196
Se(1)–Se(2)	2.322(6)	2.359	C(11)–Se(1)–Se(2)	101.99(9)	102.189
Se(2)–C(21)	1.934(3)	1.942	C(12)–C(11)–Se(1)	116.6(2)	122.547
Se(1)–O(1A)	4.640	4.675	C(22)–C(21)–Se(2)	122.7(2)	121.960
Se(2)–O(2)	3.008	2.916			

31, together with the formation of seleninic acid thiol ester **32** ($m/z 327$) and selenenic acid thiol ester **33**. In the reaction of seleninate ester with 3 equiv of PhSH we were not able to detect the peak due to selenenyl sulfide, which may be due to its fast disproportionation into diselenide and disulfide. The formation of diphenyl disulfide ($m/z 218$), seleninic acid **34** ($m/z 227$), and selenenic acid **35** ($m/z 241.00$) was observed.



31, X = OSPh; **32**, X = O₂SPh
33, X = O₃SPh; **34**, X = O₂H;
35, X = O₃H

Reaction of 16 with TBHP. When **16** (280.17 ppm) was treated with 1 equiv of TBHP, it did not show any considerable shift in ^{77}Se NMR spectrum. Reaction of **16** with 2 equiv of TBHP afforded a very weak signal at 992.76 ppm probably due to the RSe–O–allyl species, which readily disappeared upon addition of excess TBHP, and a new signal appeared at 1345.96 ppm due to cyclic seleninate ester **17** which clearly shows that 2,3-sigmatropic shift has taken place.

Crystal Structure of 15. The ORTEP diagram of compound **15** is shown in Figure 1. The important bond distances and bond angles along with the calculated values (vide infra) are given in Table 2. The most interesting feature of the structure is the presence of Se···OH intramolecular interaction. In compound **15**, the Se···O distance {Se(2)···O(2) = 3.008 Å} is shorter than the

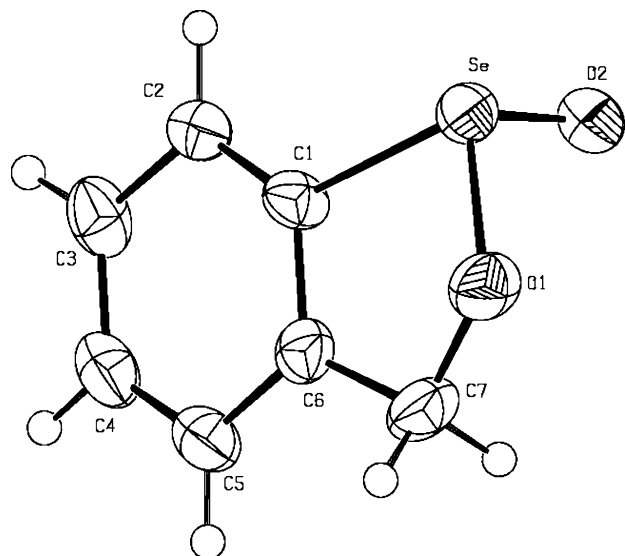


FIGURE 2. Molecular structure of **17**. Selected bond length (Å) and angles (deg): Se–O(2) 1.630(5); Se–O(1) 1.794(5); Se–C(1) 1.939(4); O(2)–Se–O(1) 105.1(3); O(2)–Se–C(1) 101.4(2); O(1)–Se–C(1) 86.5(3); C(7)–O(1)–Se 113.6(4); C(2)–C(1)–Se 127.0(5); C(6)–C(1)–Se 108.0(5).

sum of van der Waals radii (3.40 Å)³² and the O(2)–Se(2)–Se(1) angle is 166.10°, which indicates a weak nonbonded Se···OH interaction in the solid state. Interestingly, the calculated distance for such an interaction is 2.915 Å (vide infra). The short Se···O distance may also result due to Se···HO intramolecular interaction. However, in view of the observed intermolecular short H-bonding contact involving the hydroxy group, the Se···HO interaction can safely be ruled out. The other hydroxy O···Se distance is greater than the sum of the van der Waals radii [Se(1)···O(1) is 4.63 Å]. This leads to a T-shaped geometry around Se(2) and V-shaped geometry around Se(1). The C(11)–Se(1)–Se(2)–C(21) dihedral angle is –78.53(13)°, indicating a “cisoid” conformation for the diselenide.³³ In the crystal the molecules are linked by hydrogen bonds [O(1)–H(1)···O(2)#1, $d(\text{H}\cdots\text{A}) = 1.95$ Å and O(2)H(2)···O(10#2, $d(\text{H}\cdots\text{A}) = 2.00$ Å].

Crystal Structure of 17. The ORTEP diagram of **17** is shown in Figure 2. In **17**, the Se–O distance (Se–O(1) = 1.794(5) Å) is closer to the normal single bond distance of 1.774 Å found in OCS₂.³⁴ The Se=O bond distance (Se=O(2) = 1.630 Å) is shorter than that found in dicyclohexyl-*trans*-3,4-dihydroxy-1-selenolane (1.755 and 1.67 Å) where selenium atom is attached to the sp³ carbon atom [Csp³–Se(OH)–Csp³ and Csp³–Se(O)–Csp³ respectively] but closer to Se–O (1.648 and 1.646 Å) found in 3,3'-(4-chloroquinoly)selenolane and phenyl-1-bromo-2-phenylethylene selenolane where selenium atom is directly attached to the sp²-hybridized carbon atoms [Csp²–Se(O)–Csp²].³⁵

(32) Pauling, L. *The Nature of Chemical Bond*, 3rd ed.; Cornell University Press: Ithaca, NY, 1960.

(33) Sandman, D. J.; Li, L.; Tripathy, S.; Stark, J. C.; Acampora, L. A.; Foxman, B. M. *Organometallics* **1994**, *13*, 348.

(34) (a) Dahlen, B. *Acta Crystallogr.* **1973**, *B29*, 595. (b) Dahlen B.; Lindgren B. *Acta Chem. Scand.* **1973**, *27*, 2218.

(35) Dikarev, E. V.; Petrukina, M. A.; Li, X.; Block, E. *Inorg. Chem.* **2003**, *42*, 1966 and references therein.

TABLE 3. Comparison of Experimentally Obtained Structural Parameters (Å and deg) with That Computed at the MPW1PW91/LanL2DZdp, 6-311G** Level for Compound **22**

	exptl	calcd		exptl	calcd
Te(1)–C(1A)	2.135(7)	2.145	C(1B)–Te(2)–Te(1)	102.200	102.049
Te(1)–Te(2)	2.696(7)	2.728	C(1A)–Te(1)–Te(1)	99.660	99.944
Te(2)–C(1B)	2.143(7)	2.141	O(1B)–Te(2)–Te(1)	165.600	169.100
Te(2)···O(1B)	3.021	2.843			
Te(1)···O(1A)	4.781	4.827			

TABLE 4. Comparison of Experimentally Obtained Structural Parameters (Å and deg) with That Computed at the MPW1PW91/LanL2DZdp, 6-311G** Level for Compound **25**

	exptl	calcd		exptl	calcd
Te–C(1)	2.134(3)	2.137	C(1)–Te–Te#	98.69(9)	99.820
Te–Te#	2.71(5)	2.721	C(6)–C(1)–Te	123.4(2)	122.516
Cl–C(7)	1.791(4)	1.810	C(2)–C(1)–Te	116.7(2)	117.692
C(1)–C(2)	1.395(5)	1.395	Cl–C(7)–H(7A)	109.200	105.536
Cl–Te	3.974	3.947	Cl–Te–Te#	126.540	126.718

Crystal Structure of 19. The ORTEP diagram of **19** is given in the Supporting Information (Figure S45). The molecule is isostructural with related 3,3'-spirobi(3-selenaphthalide)³⁶ and crystallizes in space group *C2/c* with the selenium atom located at the inversion center. The O(1)–Se–O(1)#1 and C(1)–Se–C(1)#1 angles are 174.41(13)° and 101.74(15)°, respectively. The corresponding angles in **10** are 172.99° and 102.95°, respectively. Considering the lone pair on selenium, the geometry around selenium atom is trigonal bipyramidal with the more electronegative oxygens in the apical positions.

Crystal Structure of 22. The ORTEP diagram of compound **22** is given in the Supporting Information (Figure S46). The important bond lengths and bond angles along with the calculated values are given in Table 3. Ditelluride **22** is isostructural with the diselenide **15** and has crystallized in space group *P2(1)/n*. Similar to **15**, ditelluride **22** also exhibits novel Te···OH intramolecular interaction, leading to T-shaped geometry around Te(2) and V-shaped geometry around Te(1). The Te(2)···O(1B) distance is 3.021 Å, which is shorter than the sum of their van der Waals radii (3.6 Å). The O(1B)–Te(2)–Te(1) angle is 165.60° and indicates an almost linear arrangement for the three atoms. The C(1A)–Te(1)–Te(2)–C(1B) dihedral angle is –79.1(3)°. The molecules are linked by hydrogen bonds [O(1A)–H(1AA)···O(1B)#1 and O(1B)–H(1BA)···O(1A) #2].

Crystal Structure of 25. The ORTEP diagram of **25** is provided in the Supporting Information (Figure S47). The important bond lengths and bond angles and the corresponding calculated values are given in Table 4. The molecule has a 2-fold axis running through the center of the Te–Te bond, and hence, only half the molecule is represented as the asymmetric unit. Surprisingly, the structure does not show any Te···Cl intramolecular

(36) (a) Dahlen B. *Acta Crystallogr.* **1974**, *B30*, 647. (b) Claeson, S.; Langer, V.; Allenmark, S. *Chirality* **2000**, *12*, 71. (c) Kawashima, T.; Ohno, F.; Okazaki, R. *J. Am. Chem. Soc.* **1993**, *115*, 10434. (d) Ohno, F.; Kawashima, T.; Okazaki, R. *Chem. Commun.* **1997**, 1671. (e) Ohno, F.; Kawashima, T.; Okazaki, R. *Chem. Commun.* **2001**, 463. (f) Kano, N.; Daicho, Y.; Nakanishi, N.; Kawashima, T. *Org. Lett.* **2001**, *3*, 691 (g) Drabowicz, J.; Luczak, J.; Mikołajczyk, M.; Yamamoto, Y.; Matsukawa, S.; Akiba, K. *Tetrahedron: Asymmetry* **2002**, *13*, 2079.

TABLE 5. Comparison of Experimentally Obtained Structural Parameters (Å and deg) with that Computed at the MPW1PW91/LanL2DZdp, 6-311G** Level for Compound **28**

	exptl	calcd		exptl	calcd
Te(2)–C(1B)	2.131(5)	2.133	C(1B)–Te(2)–Te(2)#	100.66(13)	100.173
Te(2)–Te(2)#	2.693(8)	2.696	C(2B)–C(1B)–Te(2)	126.6(4)	125.668
O(2B)–C(8B)	1.425(6)	1.412	C(6B)–C(1B)–Te(2)	114.4(3)	114.525
O(2B)–H(2B)	0.840	0.956			
O(1B)–Te(2)	2.929	2.936			

interaction. The Te⋯Cl distances are ~ 3.97 Å and the Te#–Te–Cl angles (126°) deviate quite significantly from 180° , confirming the absence of any intramolecular interaction (vide infra). However, the crystal packing shows strong intermolecular Te⋯Te interaction (3.952 Å) resulting in a stacking of the molecules one over another along the *b*-axis (Supporting Information Figure S48).

Crystal Structure of 28. The ORTEP diagram of compound **28** is provided in the Supporting Information (Figure S49). The important bond lengths and bond angles and the corresponding calculated values are given in Table 5. Ditelluride **28** also crystallizes in space group *C2/c* with the inversion center situated at the center of the Te–Te bond. Interestingly, in this molecule both the ether and hydroxy groups are present. The Te(2)⋯O(1B) distance is 2.929 Å and the O(1B)–Te(2)–Te(2)# angle is 152.22° . Though the hydroxy oxygen is suitably disposed, the Te⋯OH distance is 4.612 Å and does not indicate an interaction. This observation is similar to that reported by Wirth et al. for **4b** where the Se⋯O(methoxy) was found to be 2.977 Å and the distance from the hydroxy-O was 4.22 Å. Similar to **22**, in **28** also the molecules are linked by hydrogen bonds [O(2A)–H(2AB)⋯O(2B)#3 $d(\text{H}\cdots\text{A}) = 1.89$ Å and O(2B)–H(2BB)⋯O(2A) $d(\text{H}\cdots\text{A}) = 1.89$ Å] (Figure 8). The presence of the $-\text{CH}_2-\text{CH}_2-\text{OH}$ substituent on the aryl ring results in the formation of an interesting O–H⋯O hydrogen bonding (shown in Figure S50 of the Supporting Information), where four molecules of **28** are brought together to form a O_4H_4 -suarane.

Density Functional Theory Studies

Electronic structure calculations have been carried out using the density functional theory method with an immediate objective of identifying the electronic origin as well as nature of nonbonding interactions in the present series of compounds. We have employed the hybrid density functional method, namely mPW1PW91, for this study. The mPW1PW91 method has been known to reproduce structural parameters quite well for tellurium compounds.³⁷ Introduction of electron correlation is known to be critical for an adequate representation of the closed-shell interactions.³⁸ Use of extended basis sets is desirable for achieving better agreement between experimental and calculated geometries.^{39,40} Thus, we have used the mPW1PW91/LanL2DZdp, 6-311G** level of theory for this study.

(37) Klapötke, T. M.; Krumm, B.; Mayer, P.; Schwab, I. *Angew. Chem., Int. Ed.* **2005**, *42*, 5843.

(38) Pyykkö, P. *Chem. Rev.* **1997**, *97*, 597.

(39) Minkin, V. I.; Minyaev, R. M. *Chem. Rev.* **2001**, *101*, 1247.

(40) Sanz, P.; Yáñez, O.; Mó, O. *Chem. Eur. J.* **2002**, *8*, 3999.

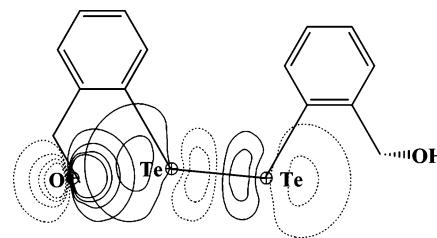


FIGURE 3. NBO contour diagram representing the $n_{\text{O}} \rightarrow \sigma^*_{\text{Te-Te}}$ orbital interaction in **22**.

The DFT calculations are found to reproduce the principal structural features of the model organochalcogens quite well. As is evident from earlier sections (Tables 2–5), the computed chalcogen⋯O distances are in good agreement with those found using X-ray crystallography. Furthermore, key geometrical features such as Se–Se and Te–Te bond lengths and C–Se–Se and O–Se–Se angles, along with other geometric parameters obtained for compounds **15**, **22**, **25**, and **28** are very much comparable with the experimentally determined values.

The nature of the chalcogen⋯O nonbonded interaction is analyzed using the natural bond orbital (NBO) method. In ditelluride **22**, with benzylic alcohol as the donor, the stabilizing interaction between tellurium and oxygen atoms primarily arises due to the $n_{\text{O}} \rightarrow \sigma^*_{\text{Te-Te}}$ orbital interaction. The NBO contour diagram for compound **22**, as given in Figure 3, clearly depicts the involvement of nonbonding orbital on oxygen atom (n_{O}) and σ^* antibonding orbital of the Te–Te unit ($\sigma^*_{\text{Te-Te}}$). The second-order perturbation energy obtained from NBO analysis conveys the effectiveness of the orbital interaction.^{41,42} The estimated value for **22** is found to be 8.75 kcal/mol, highlighting the presence of a strong nonbonding interaction between tellurium and oxygen atoms. Deletion of selected orbitals from the donor–acceptor pair is another way to substantiate the importance of nonbonding interaction.^{43a,b} It is interesting to note that the NBO *deletion energy* computed for **22** is also high, indicating a fairly good nonbonding interaction.^{43c} Further, it was noticed that the Te–Te bond undergoes only a slight elongation compared to the corresponding diphenylditelluride, computed at the same level of theory.

The magnitudes of $n_{\text{O}} \rightarrow \sigma^*_{\text{Te-Te}}$ interaction energy indicate a significant covalent interaction operating between tellurium and heteroatom. Estimated covalency factors χ for chalcogen⋯O interaction in compounds **15** and **22** are found to be 34% and 50%, respectively, at the mPW1PW91 level of theory.^{44,45} At the same time, atomic charges computed with natural population analysis⁴⁶ on

(41) The second-order perturbation energy estimates the donor–acceptor interactions. These interactions lead to a departure from idealized Lewis structure description by losing occupancy from the localized Lewis type NBOs into the empty non-Lewis orbitals (delocalization). For each donor NBO (i) and the acceptor NBO (j), the stabilization energy (E_{S}) associated with delocalization is estimated as $E_{\text{S}} = \Delta E_{ij} = q_i [F(i,j)]^2 / (\epsilon_j - \epsilon_i)$ where q_i is the donor orbital occupancy, ϵ_i and ϵ_j are orbital energies, and $F(i,j)$ is the off-diagonal NBO Fock matrix elements.

(42) Reed, A. E.; Curtiss, L. A.; Weinhold, F. *Chem. Rev.* **1988**, *88*, 899.

(43) (a) Giuffreda, M. G.; Bruschi, M.; Lüthi, H. P. *Chem. Eur. J.* **2004**, *10*, 5671. (b) Bruschi, M.; Giuffreda, M. G.; Lüthi, H. P. *Chem. Eur. J.* **2002**, *8*, 4216. (c) Deletion energy is the loss of stabilization energy due to the selective removal of the acceptor orbital helping in nonbonding interaction.

TABLE 6. Second Order Perturbation Energy and BCP Properties of **15**, **22**, and **28**

serial no.	second-order perturbation energy ^a		NPA charges		Properties of Te...O BCP ^d	
	$E_{\text{chalcogen}\cdots\text{O}}^b$	E_{del}^c	acceptor chalcogen	donor oxygen	r	$\nabla^2\rho$
15	4.04	10.42	0.23	-0.72	0.016	-0.013
22	8.75	12.25	0.35	-0.72	0.022	-0.014
29	2.50	7.10	0.33	-0.55	BCP absent	

^a All energies are calculated at the mPW1PW91/mPW1PW91/LanL2DZdp ECP, 6-311G** level and are in kcal/mol. ^b Second-order perturbation energy of $n_{\text{O}} \rightarrow \sigma_{\text{Se}(\text{Te})-\text{Se}(\text{Te})}^*$ delocalization. ^c $\sigma_{\text{Se}(\text{Te})-\text{Se}(\text{Te})}^*$ orbital deletion energy. ^d In atomic units.

chalcogens and oxygen atoms (Table 6) suggest a modest electrostatic contribution toward the nonbonding interaction.

Next, we have investigated the properties of electron density at the Te...O bond critical point (*bcp*) using Bader's theory of atoms in molecules (AIM) (Table 6).⁴⁷ The AIM formalism involves topological analysis of the properties of electron density (ρ) between interacting atoms. Chemical bonding can thus be identified by the presence of a bond critical point (*bcp*), where electron density reaches a minimum along the bond path. Distinct bond critical points associated with chalcogen...O interaction are identified in compounds **15** and **22**. The values of ρ obtained for these compounds are in a similar range as that of the neutral hydrogen bond (Table 6). The ρ values are much smaller than a covalent bond (e.g., $\rho_{\text{C-C}} = 0.24 \text{ ea}_0^{-3}$) but larger than those for the practical boundary of molecules ($\rho = 0.001 \text{ ea}_0^{-3}$). The Laplacian (∇^2) of ρ denotes the curvature of electron density in the 3D-topological space for two interacting atoms, and it is known to recover the shell structure of an atom.⁴⁸ A negative value of $\nabla^2\rho$, as in **15** and **22**, indicates a locally concentrated electron density, characteristic of a covalent interaction. Thus, both NBO and AIM methods suggest that in compounds **15** and **28** the intramolecular nonbonding interaction is dominantly covalent in nature.

A particularly interesting observation on the ditelluride **28** relates to the distance between tellurium and phenoxy oxygen, which is found to be around 2.9 Å (both experimental as well as theoretical). While the Te...O distance is good enough to be considered for the existence of nonbonding interaction, absence of a bond critical point (using topological analysis using the AIM theory) as well as very low second-order perturbation energies (using the NBO analysis) rule out the possibility of nonbonding interaction between these two atoms.

Comparison of Acceptor Abilities of Selenium and Tellurium. It is interesting to note that the

(44) The covalency factor χ for the intramolecular Te...O can be estimated by the following equation $\chi = [(R_{\text{Te}} + R_{\text{O}})_{\text{vdw}} - d_{\text{TeO}}]/[(R_{\text{Te}} + R_{\text{O}})_{\text{vdw}} - (r_{\text{Te}} + r_{\text{O}})_{\text{cov}}]$ where R and r are the van der Waals and covalent radii, respectively, and d is the distance between the two interacting atoms.

(45) Sadekov, I. D.; Minkin, V. I.; Zakharov, A. V.; Starikov, A. G.; Borodkin, G. S.; Aldoshin, S. M.; Tkachev, V. V.; Shilov, G. V.; Berry, F. J. *J. Organomet. Chem.* **2005**, *690*, 103.

(46) (a) Natural population analysis (NPA) represents the occupancies of a set of natural atomic orbitals (NAOs) for a given molecule in an arbitrary atomic orbital basis set. (b) Reed, A. E.; Weinstock, R. B.; Weinhold, F. *J. Chem. Phys.* **1985**, *83*, 735.

(47) Bader, R. F. W. *Atoms in Molecules: A Quantum Theory*; Oxford University Press: New York, 1990.

(48) Bader, R. F. W.; Fand D. *J. Chem. Theory Comput.* **2005**, *1*, 403.

optimized Te...O distance (2.843 Å) in **22** is shorter than the Se...O distance (2.915 Å) in the corresponding selenium analogue **15**. This observation is opposite to what one might anticipate on the basis of the larger size of the tellurium atom. This apparent anomaly can be explained by considering the acceptor ability of $\sigma_{\text{Te-Te}}^*$ compared to that of $\sigma_{\text{Se-Se}}^*$ orbital. In fact, computed second-order perturbation energy for ditelluride **22** was found to be more than double that of the diselenide **15** (Table 6). Another key parameter that corroborates this observation is the higher value of electron density at the chalcogen...oxygen bond critical point. The nonbonding interaction in **22** is thus evidently stronger than the corresponding diselenide **15**.

Experimental Section

Se(dtc)₂²⁵ and TeI₂⁴⁹ were prepared by reported methods. Lithiation of compounds **13** and **26** was done by the previously reported procedure with slight modification.²⁴ All of the reactions were carried out under nitrogen or argon atmosphere.

Synthesis of Di(hydroxybenzyl) Diselenide (15). Benzyl alcohol **13** (1.4 mL, 13.5 mmol) and TMEDA (3.4 mL, 27.5 mmol) were added to pentane (100 mL), and the mixture was stirred thoroughly. To that was added *n*-BuLi (17.5 mL, 28 mmol) at 0 °C. The mixture was refluxed at 50 °C for 14 h. After that lithiated product **14** settled, the dark brown colored supernatant liquid was removed, and THF (30 mL) was added to the reaction mixture. Selenium (1 g, 10 mmol) powder was added at 0 °C, and the reaction mixture was stirred for 6–7 h. The product obtained was worked up in the usual manner, extracted with methyl *tert*-butyl ether, dried over anhydrous sodium sulfate, and filtered, and 100 mg of KOH was added to that solution. Diselenide **15** was obtained after evaporation of solvent as a yellow solid (1.5 g, 60%). Recrystallization from toluene afforded yellow crystals: mp 67–68 °C; IR (KBr) 3306 (br), 2915, 2846, 1440, 1054, 1022, 739 cm⁻¹; ¹H NMR (400 MHz, CDCl₃) δ 1.85 (s, 2H), 4.7 (s, 4H), 7.2 (t, $J = 7.19$ Hz, 2H); 7.3 (t, $J = 7.23$ Hz, 2H), 7.4 (d, $J = 7.23$ Hz 2H), 7.7 (d, $J = 7.23$ Hz, 2H); ¹³C NMR (400 MHz, CDCl₃) δ 65.4, 128.46, 128.85, 128.98, 130.69, 135.07, 142.18; ⁷⁷Se NMR (300 MHz, CDCl₃) δ 428; ES MS m/z 368.282 (M⁺, 30). Anal. Calcd for C₁₄H₁₄Se₂O₂: C, 45.16; H 3.76. Found: C, 44.96; H, 3.52.

Allyl (2-Hydroxybenzyl) Selenide (16). Sodium borohydride (0.25 g, 6.72 mmol) was added to an ice-cooled solution of **15** (0.5 g, 1.34 mmol) in absolute ethanol (25 mL). Once the addition was complete, the ice bath was removed and the reaction mixture was stirred at room temperature for 30 min. Allyl bromide (1.5 mL, 5.36 mmol) was added to the clear colorless reaction mixture, and stirring was continued overnight. The reaction mixture was poured into 100 mL of ether, washed with a saturated solution of NH₄Cl and NaCl and with water. It was dried over sodium sulfate and solvent was evaporated in a vacuum. The residue was chromatographed (elution with 10% ethyl acetate–petroleum ether) to afford **16** as a colorless liquid (0.3 g, 50%): IR (neat) 3356, 3058, 2927, 1632, 1439, 1195, 1026, 751 cm⁻¹; ¹H NMR (400 MHz, CDCl₃) δ 3.4 (d, $J = 7.22$ Hz, 2H), 4.7 (s, 2H), 4.9 (m, 2H), 5.9 (m, 1H), 7.2 (t, $J = 7.32$ Hz, 1H), 7.1 (t, $J = 7.42$ Hz, 1H), 7.28 (d, $J = 7.32$ Hz, 1H), 7.45 (d, $J = 8.54$ Hz, 1H); ¹³C NMR (400 MHz, CDCl₃) δ 142.8, 134.33, 134.27, 129.56, 128.53, 128.2, 127.8, 117.2, 65.0, 30.8; ⁷⁷Se NMR (500 MHz, CDCl₃) δ 280.11; ES-MS m/z 227 (M⁺, 12), 211 (28), 128 (47), 130 (100); exact mass calcd for C₁₀H₁₂OSe 227.0713, found 227.0487.

Benzo-1,2-oxaselenolane Se-Oxide (17). TBHP (1.55 mL of a 70% aqueous solution, 12.16 mmol) was added to a solution

(49) Brauer, G. *Handbook of Preparative Inorganic Chemistry*; Academic Press: New York, 1962; Vol. 1, p 433.

of allyl (benzyl alcohol) selenide (0.46 g, 2.03 mmol) in 30 mL of dichloromethane, and the reaction mixture was stirred at room temperature for 6 h. The mixture was concentrated under vacuum, and the residue was chromatographed (elution with 10% methanol–ethyl acetate) to afford **17** as white powder (0.25 g, 61%). Crystallization from dichloromethane/hexane (1:1) afforded colorless needle shaped crystals: mp 139–140 °C; IR (KBr) 3077, 2915, 2858, 1435, 1199, 975, 859, 771, 553 cm^{-1} ; ^1H NMR (400 MHz, D_2O) δ 5.6 (d, 1H), 6.00 (d, $J = 4.88$ Hz, 1H), 7.5 (m, 2H), 7.6 (t, $J = 7.63$ Hz, 1H), 7.8 (d, $J = 0.61$ Hz, 1H); ^{13}C NMR (400 MHz, CDCl_3) δ 78.31, 122.67, 125.97, 129.20, 132.19, 143.52, 147.0; ^{77}Se NMR (500 MHz, CDCl_3) δ 1352.49; ES-MS m/z 202.9 (M^+ , 38), 184 (10), 156.9 (100), 82.9 (62.6). Anal. Calcd for $\text{C}_7\text{H}_6\text{O}_2\text{Se}$: C, 41.83; H, 3.009. Found: C, 42.02; H, 3.17.

The same product was obtained in 70% yield from the similar oxidation of bis(benzyl alcohol) diselenide **15** (0.5 g, 1.344 mmol) with H_2O_2 (0.5 mL of a 30% aqueous solution, 4.4 mmol) in dioxane at 0 °C for 30 min. Compound was recrystallized from water to furnish a white powder (0.35 g, 70%).

Di(2-hydroxybenzyl) Selenide (18). To a suspension of dilithiated derivative **14** (26 mmol) in THF was added $\text{Se}(\text{dte})_2$ (5.3 g, 13 mmol) at 0 °C under a brisk flow of nitrogen. The reaction mixture was stirred for 6 h and poured into a beaker containing 100 mL of a cold saturated solution of sodium bicarbonate. The resulting organic layer and the dichloromethane extracts from the aqueous layer were combined, dried over sodium sulfate, and concentrated in a vacuum to give a dark viscous oil. Crystallization of this compound from dichloromethane/hexane (1:1) afforded **18** as light yellow needles (1.5 g, 39%): mp 86–87 °C; IR (KBr) 3325, 1461, 1006, 749 cm^{-1} ; ^1H NMR (400 MHz, CDCl_3) δ 2.00 (s, 2H), 4.8 (s, 4H), 7.2 (t, $J = 7.32$ Hz, 2H); 7.28 (m, 4H), 7.5 (d, $J = 7.32$ Hz, 2H); ^{13}C NMR (400 MHz, CDCl_3) δ 65.3, 128.3, 128.9, 129.2, 130.4, 134.4, 142.1; ^{77}Se NMR (500 MHz, CDCl_3) δ 325.39; ES-MS m/z 293.03 (45, M^+), 245.01 (25), 136.03 (60), 91.07(100); exact mass calcd for $\text{C}_{14}\text{H}_{14}\text{O}_2\text{Se}$ 293.00, found 293.03. Anal. Calcd for $\text{C}_{14}\text{H}_{14}\text{O}_2\text{Se}$: C, 57.37; H, 4.81. Found: C, 57.38; H, 4.87.

1,1'-Spiro[3H-2,1-benzoxaselenolene] (19). Hydrogen peroxide [(30%) 0.1 g, (0.33 mL, 2.9 mmol)] was added dropwise with cooling and stirring to a solution of bis(benzyl alcohol) selenide **18** (0.5 g, 1.7 mmol) in 20 mL of acetic acid. After the addition, the temperature of the reaction mixture was allowed to rise to room temperature. The mixture was stirred for 30 min at room temperature. The solvent was evaporated in vacuo to 2 mL and kept aside to give colorless crystals of **19** (0.3 g, 60%): mp 169–170 °C; IR (KBr) 3049, 2871, 2814, 1439, 1202, 1038, 1014, 773 cm^{-1} ; ^1H NMR (400 MHz, CDCl_3) δ 8.02 (d, $J = 7.32$ Hz, 2H), 7.41 (m, 4H), 7.22 (d, $J = 8.54$ Hz, 2H), 5.3 (s, 4H); ^{13}C NMR (400 MHz, CDCl_3) δ 143.47, 133.83, 130.90, 127.99, 127.75, 124.07, 70.93; ^{77}Se NMR (400 MHz, CDCl_3) δ 816.8; ES-MS m/z 292.8 (M^+ , 10), 231 (10), 165 (100), 152.05 (33.3), 128.08 (18), 115.04 (20); exact mass calcd for $\text{C}_{14}\text{H}_{12}\text{O}_2\text{Se}$: 291, found 292.89. Anal. Calcd for $\text{C}_{14}\text{H}_{12}\text{O}_2\text{Se}$: C, 57.73; H, 4.12. Found: C, 57.88; H, 4.32.

Selenenyl Sulfide (20). Pentanethiol (100 μL , 80 mM) was added to a solution of **17** (50 mg, 0.25 mM) in dichloromethane (5 mL), and the mixture was stirred at room temperature for 10 min. The mixture was chromatographed by preparative TLC using hexane/dichloromethane (1:1) to afford the product as pale yellow oil (55 mg, 81%): IR (neat) 3377, 1452, 1023, 750 cm^{-1} ; ^1H NMR (400 MHz, CDCl_3) δ 7.89–7.26 (m, 4H), 4.82 (s, 2H), 2.81 (t, 2H), 2.00 (b, 1H), 1.6 (m, 2H), 1.25 (m, 2H), 0.85 (t, 3H); ^{13}C NMR (400 MHz, CDCl_3) δ 142.0, 132.57, 131.73, 128.75, 128.05, 65.58, 38.29, 30.74, 30.03, 22.40, 14.10; ^{77}Se NMR (500 MHz) δ 438.23.

Selenenyl Sulfide (21). Benzenethiol (20 μL , 0.199 mmol) was added to the solution of oxaselenane **17** (10 mg, 0.049 mmol) in 0.5 mL of CDCl_3 , and the mixture was shaken for 2 min. The color of the reaction mixture immediately turned

from colorless to yellow. We were unable to isolate the product in pure form but we characterized it *in situ*: IR (KBr) 3388, 1472, 1018, 741 cm^{-1} ; ^1H NMR (400 MHz, CDCl_3) δ 7.78–7.79 (m), 7.76–7.746 (m), 7.34–7.20 (m), 4.77 (s, 2H), 3.43 (s, SH), 1.78 (b, OH); ^{77}Se NMR (500 MHz) δ 506.

Di(2-hydroxybenzyl) Ditelluride (22). Benzyl alcohol (1.4 mL, 13.5 mmol) and TMEDA (3.4 mL, 25 mmol) were added to pentane (100 mL), and the mixture was stirred. To that mixture was added *n*-BuLi (18.2 mL, 20 mmol) at 0 °C. The mixture was refluxed at 50 °C for 14 h. The lithiated product was precipitated. The supernatant solvent pentane was removed, and THF (30 mL) was added to the reaction mixture. Tellurium powder (1 g) was added at 0 °C and the mixture stirred for 6–7 h. The product obtained was worked up in the usual manner, extracted with dichloromethane, dried over anhydrous sodium sulfate, and filtered. Dark red **17** was obtained after evaporation of the filtrate. Recrystallization from dichloromethane afforded red crystals: yield 1.5 g, 50%; mp 65–68 °C; IR (KBr) 3342, 1577, 1439, 1202, 1040, 1008, 755 cm^{-1} ; ^1H NMR (400 MHz, $\text{DMSO}-d_6$) δ 4.6 (s, 4H), 5.8 (s, 2H), 7.05 (t, $J = 7.32$ Hz, 2H), 7.25 (m, 4H) 7.8 (d, $J = 7.32$ Hz, 2H); ^{13}C NMR (400 MHz, CDCl_3) δ 66.2, 109.3, 127.0, 127.3, 128.4, 138.6, 143.9; ^{125}Te NMR (300 MHz, CDCl_3) δ 301; ES-MS m/z 470 (M^+ , 100). Anal. Calcd for $\text{C}_{14}\text{H}_{14}\text{Te}_2\text{O}_2$: C, 35.820; H, 3.006. Found: C, 35.92; H, 3.13.

Tellurinate Ester (24). The ester **24** was obtained in 70% yield by reaction of **22** (0.5 g, 1.344 mmol) with H_2O_2 (0.5 mL of a 30% aqueous solution, 4.4 mmol) in dioxane (20 mL) at 0 °C for 30 min. The solvent was evaporated and the crude product recrystallized from CH_2Cl_2 /methanol to give a white product (0.35 g, 70%): mp 200 °C dec; IR (KBr) 3055, 2909, 2822, 1439, 1049, 1036, 741, 641 cm^{-1} ; ^1H NMR (400 MHz, CDCl_3) δ 7.3–7.6 (m, 4H), 5.2 (m, 2H); ^{13}C NMR (400 MHz, $\text{DMSO}-d_6$) δ 66.39, 126.43, 128.06, 129.18, 132.36, 141.3, 142.54; ^{125}Te NMR (500 MHz), δ 922; ES-MS m/z 250 (M^+ , 40). Anal. Calcd for $\text{C}_7\text{H}_6\text{O}_2\text{Te}$: C, 33.66; H, 2.42. Found: C, 34.01; H, 2.81.

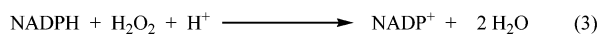
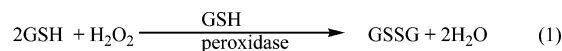
Synthesis of Di(2-chlorobenzyl) Ditelluride (25). Ditelluride **22** (2.0 g, 5.4 mmol) and pyridine (1.2 mL, 16 mmol) were taken in dichloromethane (100 mL). Thionyl chloride (1 mL, 13.5 mmol) was then slowly added to the solution at 0 °C under nitrogen atmosphere. The mixture was stirred for 4 h at room temperature, after which an excess amount of 2 N HCl was added. After the usual extraction with dichloromethane a dark red crude product was obtained. Recrystallization from hexane/ CH_2Cl_2 as eluent) afforded **25** as red crystals (0.7 g, 25%): mp 50–52 °C; IR (KBr) 2930, 2861, 1685, 734, 664 cm^{-1} ; ^1H NMR (300 MHz, CDCl_3) δ 4.7 (s, 4H), 7.1 (t, $J = 7.69$ Hz, 2H), 7.25 (m, 2H), 7.35 (d, $J = 7.69$ Hz, 2H) and 8.0 (d, $J = 7.69$ Hz, 2H); ^{125}Te NMR (300 MHz, CDCl_3) δ ; m/z 507.85 (M^+ , 50). Anal. Calcd for $\text{C}_{14}\text{H}_{12}\text{Te}_2\text{Cl}_2$: C, 33.21; H, 2.38. Found: C, 33.0; H, 2.52.

Di(2-phenoxyethanol) Ditelluride (28). To 2-phenoxyethanol (2.6 mL, 21 mmol) in hexane/pentane (50 mL) was added *n*-BuLi (1.6 M, 28 mL, 45 mmol) dropwise at –78 °C, and the reaction mixture was allowed to come to room temperature. The resulting solution was stirred for 24 h at this temperature. The solvent was removed, and 30 mL of dry THF was added to the lithiated product. Tellurium powder (2.7 g, 21 mmol) was added at 0 °C under a brisk flow of nitrogen, and the solution was stirred for 12 h at room temperature and then poured into a beaker containing 100 mL of saturated NH_4Cl solution. The organic layer and the dichloromethane extract from the aqueous layer were combined and dried over sodium sulfate, and solvent was evaporated in vacuo to afford 1.0 g of the crude product which was recrystallized from THF/hexane to give 1 g (20% yield) of yellow crystalline product: mp 165–166 °C; IR (KBr) 3255 (br), 2920, 2870, 1437, 1229, 1056, 750 cm^{-1} ; ^1H NMR (400 MHz, CDCl_3) δ 3.78 (t, $J = 5.01$ Hz 4H), 4.12 (t, $J = 5.19$ Hz, 4H), 4.94 (br, 2H), 6.82 (m, 2H), 6.9 (d, $J = 7.47$ Hz, 2H), 7.25 (t, $J = 7.12$ Hz, 2H), 7.45 (d, $J = 7.63$ Hz, 2H); ^{13}C NMR (400 MHz,

CDCl₃) δ 59.67, 70.87, 97.46, 111.39, 122.84, 129.43, 136.73, 158.13; ¹²⁵Te NMR (300 MHz, DMSO) δ 163; ES-MS *m/z* 529.95 (M⁺, 100). Anal. Calcd for C₁₆H₁₈O₄Te₂: C, 36.294; H, 3.426. Found: C, 36.23; H, 3.47.

X-ray Crystallography. The diffraction measurements for compounds **15**, **22**, **25**, and **28** were performed on a Bruker P4 and for **17** and **19** on a Stoe IPDS at room temperature with graphite-monochromated Mo Kα radiation (λ = 0.7107 Å). The structures were solved by direct methods and full-matrix least-squares refinement on F² (program SHELXL-97).⁵⁰ Hydrogen atoms were localized by geometrical means. A riding model was chosen for refinement. The isotropic thermal parameters of the H atoms were fixed at 1.5 times (CH₃ groups) or 1.2 times *U*(eq) (Ar–H) of the corresponding C atom. Some details of the refinement are given in Tables S4 and S5 of the Supporting Information.

Coupled Reductase Assay. The GPx-like activity of **6**, **8**, and **15–19** was measured according to the literature method²⁷ using ebselen **5** as a standard. The reaction was carried out at 37 °C in 0.7 mL of the solution containing 50 mM potassium phosphate buffer, pH 7.0, 1 mM diethylenetriaminepentaacetic acid (DTPA), 1 mM GSH, 0.1 mmol of NADPH, 0.6 unit of glutathione reductase, 2.5 μM of catalyst, and 0.5 mmol of H₂O₂. The activity was followed by the decrease of NADPH absorption at 340 nm (eqs 1–3). Appropriate controls were carried out without catalyst and subtracted. The consumption of NADPH in the absence of test catalysts (control) was 1.734 × 10⁻⁵ M NADPH/min. The initial reduction rate and activity are expressed in M/min of NADPH concentration and μmoles of NADPH utilized per minute per μmole, respectively.



Computational Methods

All geometries were optimized using analytical gradient techniques implemented in the Gaussian98 suite of quantum chemical program.⁵¹ All stationary points were characterized as minima by evaluating Hessian indices on respective potential energy surfaces. For the tellurium systems, relativistic effects are known to be nontrivial, and thus we used a basis set consisting of quasirelativistic effective core potentials (ECPs).⁵² LanL2DZ^{dp} ECP was employed for tellurium centers. This is the Hay–Wadt's ECP plus valence basis functions⁵³ with extra diffuse and polarization functions for *p*-block

(50) (a) Sheldrick, G. M. *SHELXS 97, Program for Crystal Structures Solution*; University of Gottingen: Gottingen, Germany, 1990. (b) Altomare, A.; Burla, M. C.; Camalli, M.; Cascarano, G. L.; Giacovazzo, C.; Guagliardi, A.; Moliterni, A. G. G.; Polidori, G.; Spagna, R. *J. Appl. Crystallogr.* **1999**, *32*, 115. (c) Sheldrick, G. M. *SHELXL 97, Program for Crystal Structures Refinement*; University of Gottingen: Gottingen, Germany, 1997.

(51) Frisch et al. *Gaussian 98*, revision A.6; Gaussian, Inc.: Pittsburgh, PA, 1998.

(52) Huzinaga, S. *Gaussian Basis Sets for Molecular Calculation*; Elsevier: Amsterdam, 1984.

(53) (a) Wadt, W. R.; Hay, P. J. *J. Chem. Phys.* **1985**, *82*, 284. (b) Hay, P. J.; Wadt, W. R. *J. Chem. Phys.* **1985**, *82*, 299.

elements.⁵⁴ All other elements are represented with the 6-311G** basis set. Electron correlations are partly incorporated by using Adamo and Barone's mPW1PW91 density functional, i.e., PW91 correlation combined with 25:75 mixture of Hartree–Fock and PW91 exchange for better reproduction of long-range effects.⁵⁵ Natural bond orbital (NBO) analysis was performed at the same level of theory to quantify the extent of electron delocalizations contributing to the nonbonding interaction.⁴² The nature of nonbonded interactions was further analyzed by inspecting properties of the bond critical points between tellurium and heteroatoms within Bader's Atoms in Molecule (AIM) framework, using the AIM2000 package.⁵⁷

Conclusions

Organo dichalcogenides (**15** and **22**) having hydroxy group ortho to selenium/tellurium with weak intramolecular chalcogen⋯OH interactions have been structurally characterized. The structural and theoretical studies indicate that tellurium is a better acceptor for n_O → σ*_{Te}-type interactions. Ditelluride **22** could be easily converted to the corresponding chloro derivative. Surprisingly, the structure and theoretical studies of **25** establish that there is no intramolecular Te⋯Cl interaction. Dichalcogenides **15** and **22** can easily be converted to respective esters. The seleninate esters **17**, diselenide **15**, and spirocyclic **19** exhibit good GPx-like antioxidant activity. Selenide **18** could be easily be converted to the spirocyclic compound **19**. The spirocyclic compound shows relatively poor GPx-like activity. Ditelluride **28** having both a phenoxy and a hydroxy group has been prepared. Though single-crystal X-ray diffraction studies indicate a short contact between Te⋯O (phenoxy), the AIM calculations do not support the presence of such an interaction.

Acknowledgment. We are grateful to the Department of Science and Technology (DST), New Delhi, and Council of Scientific and Industrial Research (CSIR), New Delhi, for funding this work. D.R. thanks CSIR New Delhi for a junior research fellowship. We thank IIT Bombay computer center for the computing facilities.

Supporting Information Available: ⁷⁷Se and ¹²⁵Te NMR spectra, ES-MS, tables of activity data, ORTEP diagrams of compounds **19**, **22**, **25**, and **28**, tables of crystal and refinement data, DFT-optimized geometries, energies, and figures. This material is available free of charge via the Internet at <http://pubs.acs.org>.

JO051309+

(54) Check, C. E.; Faust, T. O.; Bailey, J. M.; Wright, B. J.; Gilbert, T. M.; Sunderlin, L. S. *J. Phys. Chem. A* **2001**, *105*, 8111.

(55) Adamo, C.; Barone, V. *J. Chem. Phys.* **1998**, *108*, 664.

(56) NBO 5.0 Program., Glendening, E. D.; Badenhoop, J. K.; Reed, A. E.; Carpenter, J. E.; Bhojann, J. A.; Morales, C. M.; Weinhold, F. Theoretical Chemistry Institute, University of Wisconsin, Madison, 2001.

(57) Biegler-Konig, F.; Schonbohm, J.; Bayles, D. *J. Comput. Chem.* **2001**, *22*, 545.